

## $\sigma$ -Aromaticity and $\sigma$ -Antiaromaticity in Saturated Inorganic Rings

Zhen-Hua Li,<sup>†</sup> Damian Moran,<sup>‡</sup> Kang-Nian Fan,<sup>\*,†</sup> and Paul von Ragué Schleyer<sup>\*,‡</sup>

Center for Theoretical Chemical Physics, Laboratory of Molecular Catalysis & Innovative Material Department of Chemistry, Fudan University, Shanghai 200433, China, and Center for Computational Chemistry (CCC), University of Georgia, Athens, Georgia 30602-2525

Received: April 2, 2004; In Final Form: February 26, 2005

The magnetic properties of a series of inorganic saturated rings, (SiH<sub>2</sub>)<sub>n</sub>, (GeH<sub>2</sub>)<sub>n</sub>, (NH)<sub>n</sub>, (PH)<sub>n</sub>, (AsH)<sub>n</sub>, O<sub>n</sub>, S<sub>n</sub>, and Se<sub>n</sub> ( $n = 3-6$ ), exhibit zigzag behavior with ring size resembling that of aromatic and antiaromatic Hückel  $\pi$ -systems and (CH<sub>2</sub>)<sub>n</sub> rings. Computed GIAO-SCF nucleus-independent chemical shifts (NICS) and localized (LMO) NICS analysis indicate that the  $\sigma$ -ring electrons are chiefly responsible for this zigzag behavior. This evidence for  $\sigma$ -aromaticity is further supported by theoretical strain energy (TSE). The Hückel  $4n + 2/4n$  aromaticity/antiaromaticity rule for  $\pi$ -electron systems applies well to the smaller saturated rings.

### Introduction

Aromaticity remains a central concept in organic chemistry,<sup>1,2</sup> and its applicability to inorganic compounds is becoming ever more apparent. The recent recognition of the aromaticity of clusters of metal atoms is a prominent example.<sup>3,4</sup> However, aromaticity, like strain, electronegativity, bond order, atomic charge, and many other highly useful chemical concepts, is a virtual quantity, which cannot be measured directly experimentally. Evaluations of aromaticity using criteria with a secure physical basis typically depend on the choice of the frame of reference.<sup>1,2,5</sup> Statistical analysis of a large number of  $\pi$ -electron systems shows that the three major types of aromaticity indices, structural, energetic, and magnetic, contain similar information and show significant collinearity.<sup>2,6</sup> The nucleus-independent chemical shifts at ring centers [NICS(0)]<sup>7</sup> or 1 Å above [NICS(1)]<sup>8</sup> are newer magnetic indices that, due to their simplicity and broad applicability to a wide range of molecules, have been applied extensively since their introduction in 1996. Significantly negative NICS values generally correspond to diatropic (aromatic) behavior, whereas positive NICS characterize their paratropic (antiaromatic) counterparts. There is good qualitative agreement between ring current density maps and NICS.<sup>9</sup> NICS, as well as other indices that vary in a zigzag pattern with the total number of  $\pi$ -electrons in the series of annulene rings, provides strong corroborating evidence for alternating aromatic and antiaromatic Hückel behavior, i.e. molecules with  $4n + 2$   $\pi$ -electrons are aromatic whereas those with  $4n$   $\pi$ -electrons are antiaromatic.<sup>10</sup>

It was once assumed that only the higher energy  $\pi$ -electrons of cyclic conjugated molecules were capable of sufficient delocalization to be responsible for the special properties associated with aromaticity. Cyclopropane was recognized by Dewar to be an exception;<sup>11</sup> he attributed its “ $\sigma$ -aromaticity” to the delocalization of the ring electrons.<sup>5b</sup> Considerable theoretical evidence, both magnetic and energetic, has firmly established the  $\sigma$ -aromaticity of cyclopropane.<sup>11d</sup> For example, the strain

energy of cyclopropane is abnormally low compared to cyclobutane and to cyclotrisilane.<sup>12</sup> Still, the Walsh sp<sup>2</sup> hybridized-CH<sub>2</sub> model of cyclopropane bonding could be invoked to defend the traditional view, but with the p-orbitals in the ring plane rather than being perpendicular. But hydrogen has no energetically accessible p-orbitals, and an H<sub>6</sub> ring, constrained to  $D_{6h}$  symmetry, shows benzene-like magnetic aromaticity characteristics, which can only be due to the six delocalized  $\sigma$ -electrons in the  $\sigma$ -orbitals formed by hydrogen s atomic orbitals.<sup>13</sup> The Hückel  $4n + 2/4n$  electron rule for aromaticity/antiaromaticity also was applicable to other  $D_{nh}$  hydrogen rings.<sup>13</sup>

Unlike the extensively studied cyclic  $\pi$ -electron systems, where the changes of various aromaticity criteria with ring size generally follow the Hückel  $4n + 2/4n$  rule,<sup>1,10</sup> the first systematic study of the possible aromaticity and antiaromaticity of the saturated ring series only was published very recently.<sup>14</sup> This investigation demonstrated that the Hückel rule was followed for the smaller cycloalkanes. Since cyclopropane already had been well-established to be  $\sigma$ -aromatic, four-membered ring (4MR) systems were the focus of attention. Prior evidence concerning cyclobutane was restricted to its unexpectedly high strain energy and some magnetic anomalies. For example, while the <sup>13</sup>C and <sup>1</sup>H chemical shifts of cyclopropane are shielded, they are deshielded in cyclobutane.<sup>15</sup> The new evidence, based on NICS and NMR computations on saturated hydrocarbons, confirmed that three-membered rings (3MRs) are diatropic, but established that four-membered rings (4MRs) are paratropic.<sup>14,16</sup> Dissected NICS<sup>8,14,17</sup> analysis on the series of saturated cyclic hydrocarbons [(CH<sub>2</sub>)<sub>n</sub>,  $n = 3-10$ ] showed that the zigzag behavior of the total NICS(0) values for  $n = 3-6$  is parallel to the contributions of the  $\sigma$ -CC bonds of the ring, while the contributions of the CH bonds are additive, monotonic, and always diatropic.<sup>14</sup> Even though CH<sub>2</sub> groups involve carbon p-orbitals perpendicular to the ring, these do not combine to give Hückel-like behavior.

We now report the NICS analysis of saturated inorganic rings, comprised of main group 14, 15 (pictogen), and 16 (chalcogen) elements: (AH<sub>2</sub>)<sub>n</sub>, (A = Si, Ge), (AH)<sub>n</sub> (A = N, P, As), and A<sub>n</sub> (A = O, S, Se), where  $n = 3-6$ .<sup>18</sup> The analysis reveals zigzag NICS variation with ring size that is due chiefly to cyclic  $\sigma$ -electron delocalization. Furthermore, the magnetic evidence

\* Corresponding authors. K.-N.F.: phone, (86)21-65643977; fax, (86)-21-65643977; e-mail, knfan@fudan.edu.cn. P.v.R.S.: phone, (+1) 706 542 7510; fax, (+1) 706 542 7514; e-mail, schleyer@chem.uga.edu.

<sup>†</sup> Fudan University.

<sup>‡</sup> University of Georgia.

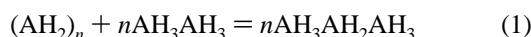
for  $\sigma$ -aromaticity in these inorganic saturated rings is further supported by their strain energies (SE).

### Computational Details

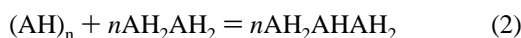
Geometries were optimized at B3LYP/6-311+G(d,p) and B3LYP/6-311+G(3df,2p) hybrid DFT levels<sup>19</sup> using the Gaussian98 program.<sup>20</sup> The global minima were established after extensive searches of alternative geometries. Harmonic vibrational frequencies at B3LYP/6-311G(d,p) established the character of all stationary points and were scaled by 0.990 to give the zero-point energies (ZPEs).<sup>21</sup> The cyclic O<sub>5</sub> geometry was optimized at QCISD/6-311G(d);<sup>22</sup> the harmonic vibrational frequencies were calculated at HF/6-311G(d), since only a weakly bound complex of O<sub>2</sub> and O<sub>3</sub> existed at B3LYP levels. The grid used for all the DFT calculation is a pruned (99, 590) grid.

In addition to the global minima, we also considered constrained geometries.  $D_{nh}$  symmetry, imposed to enforce strict  $\sigma$ - $\pi$ -separation, is a reasonable approximation for (SiH<sub>2</sub>)<sub>n</sub>, (GeH<sub>2</sub>)<sub>n</sub>, and the smaller chalcogen rings, since the energies of these restricted forms are not high relative to the global minima. However, the planar  $D_{nh}$  forms of many of the pycogen and the larger chalcogen rings suffer from wave function instability; as a consequence, the computed magnetic properties are unreliable and have not been reported. Hence, our second set of pycogen rings had imposed  $C_{nv}$  symmetry with all the hydrogens on the same side of the planar heavy atom ring. The results on all these constrained geometries are reported in the Supporting Information.

Total strain energies (TSE) at 0 K were calculated for saturated inorganic rings (lowest energy conformers) at the B3LYP/6-311+G(3df,2p) level using the following homodesmotic reactions:<sup>23</sup>



for A = Si and Ge



for A = N, P, and As



for A = O, S, and Se

NICS values using the gauge-individual atomic orbitals (GIAO) method<sup>24</sup> at the B3LYP/6-311+G(3df,2p)//B3LYP/6-311+G(3df,2p) level were computed with Gaussian98.<sup>20</sup> Dissected localized MO (LMO) NICS were computed by the individual gauge for localized orbitals (IGLO) method<sup>25</sup> at the PW91/IGLO-III//B3LYP/6-311+G(d,p) level with the deMon NMR program.<sup>26</sup> NICS(0) values are in the geometric ring centers and NICS(1) values are 1 Å along the principle (z) axis perpendicular to the average heavy atom plane. When there are two values of NICS(1) (on opposite sides of nonplanar rings; see the Supporting Information), these are quite close to one another and only their average is discussed below. The NICS(0)<sub>zz</sub> and NICS(1)<sub>zz</sub> tensor components<sup>27</sup> also were computed. Again, only the average NICS(1)<sub>zz</sub> is discussed.

### Results and Discussion

**NICS Values and Dissected NICS Analysis.** Total NICS values of all the species calculated both by GIAO and by the IGLO LMO dissection method are available in Tables S2–S9 of the Supporting Information.

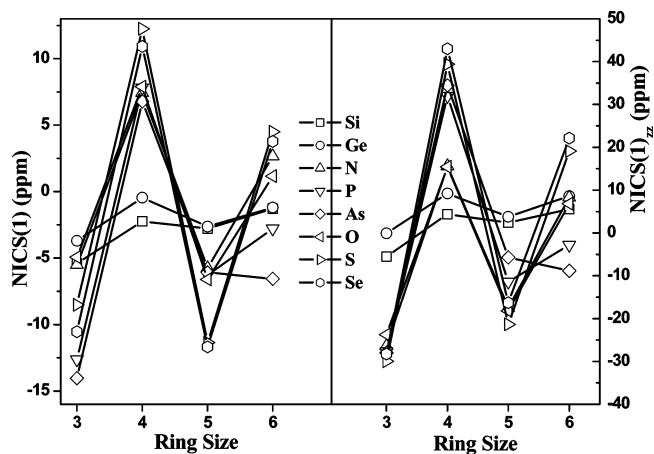


**Figure 1.** Correlation of (a) NICS(1) and (b) NICS(1)<sub>zz</sub> (calculated at the GIAO-B3LYP/6-311+G(3df,2p)//B3LYP/6-311+G(3df,2p) level) versus ring size.

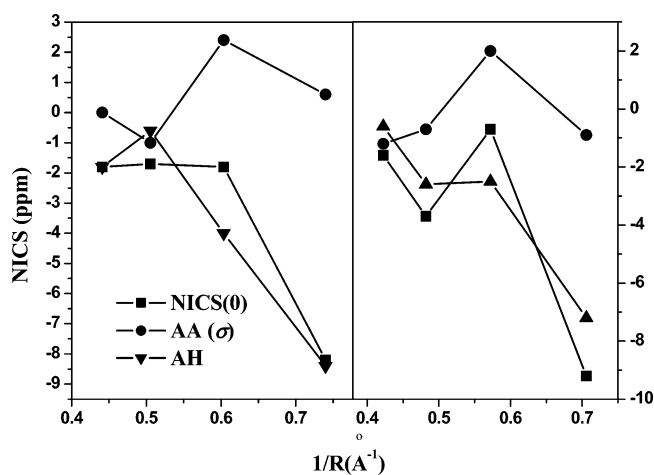


**Figure 2.** NICS at the ring center of (SiH<sub>2</sub>)<sub>n</sub> (left) and (GeH<sub>2</sub>)<sub>n</sub> (right) versus 1/R (where R is the average distance between the ring center and the Si atoms). NICS(0), LMO contributions of SiSi/GeGe bonds and SiH/GeH bonds calculated with the PW91/IGLO-III//B3LYP/6-311+G(d,p) method are shown.

The total GIAO NICS(1) vs ring size plot (Figure 1, left) reveals pronounced zigzag variations [those for (SiH<sub>2</sub>)<sub>n</sub> and (GeH<sub>2</sub>)<sub>n</sub> are dampened considerably]. Such alternating NICS(1) behavior follows the Hückel 4n + 2e rule, counting the number of  $\sigma$ -electrons of the ring bonds. NICS(1) of the groups 15 and 16 3MRs are highly negative, while those of the 4MRs are very positive. NICS(1) of the five-membered rings (5MRs) are quite negative, but those for the six-membered rings (6MRs) become more positive. It has been suggested that the NICS<sub>zz</sub> tensor component (describing the response to an external magnetic field perpendicular to the ring) should reflect the ring current more accurately.<sup>28</sup> While NICS<sub>zz</sub> is found to be a good measure of  $\pi$ -aromaticity and antiaromaticity, comparison of parts a and b of Figure 1 shows that the NICS(1) index gives very similar ring size trends. The same is true of the total GIAO NICS(0) values (see the Supporting Information for details).

We focus here on the results of the IGLO LMO NICS(0) dissections. These give the contributions of the ring AA  $\sigma$ -bonds, those of AH  $\sigma$ -bonds, and the lone pairs. (The core electron contributions are negligible.) The plots in Figures 2–4 reveal the trends in the LMO details of the NICS behavior. Note that these plots are versus 1/R, i.e., in the reverse order of ring size.

While there are small zigzag SiSi and GeGe bond trends (Figure 2), the dissected AH NICS contributions are larger in

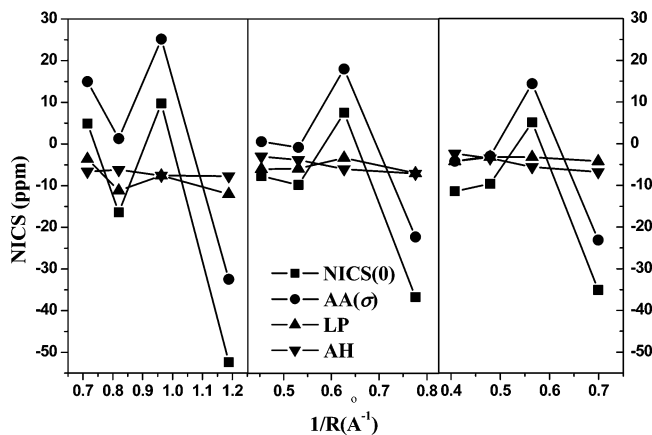


**Figure 3.** NICS at the ring center of  $(\text{NH})_n$  (left),  $(\text{PH})_n$  (middle), and  $(\text{AsH})_n$  (right) versus  $1/R$  (where  $R$  is the average distance between the ring center and the ring atoms). NICS(0), contributions of NN/PP/AsAs bonds, lone pairs (LP), and NH/PH/AsH bonds calculated with the PW91/IGLO-III/B3LYP/6-311+G(d,p) method are shown.

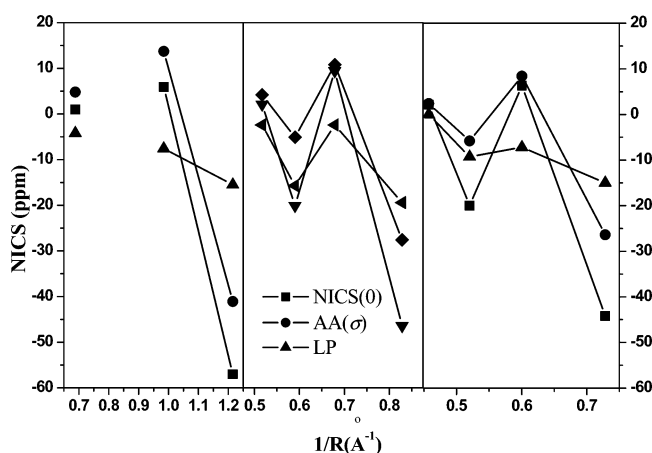


**Figure 4.** NICS at the ring center of  $\text{O}_n$  (left),  $\text{S}_n$  (middle), and  $\text{Se}_n$  (right) versus  $1/R$  (where  $R$  is the average distance between the ring center and the ring atoms). The LMO NICS(0) contributions of OO/SS/SeSe bonds as well as the lone pair (LP) sums are calculated with the PW91/IGLO-III/B3LYP/6-311+G(d,p) method.

magnitude and largely determine the total NICS(0) values, which are always diatropic.

The much larger magnitude and more pronounced zigzag NICS(0) variations of the pycogen ( $A = \text{N}, \text{P}, \text{As}$ ) series of  $(\text{AH})_n$  rings (Figure 3) are due almost entirely to the  $\text{AA}(\sigma)$  NICS(0) contributions. The  $\sigma$ -NH,  $\sigma$ -PH, and  $\sigma$ -AsH effects are insignificant and the fluctuations of the lone pair electron contributions are very small.

The  $\text{OO}(\sigma)$ ,  $\text{SS}(\sigma)$ , and  $\text{SeSe}(\sigma)$  contributions also dominate the zigzag NICS(0) behavior of the  $A_n$  chalcogen rings (Figure 4). As each O, S, and Se atom has two lone pairs,  $\pi$ -type orbitals very similar to those in the Hückel annulene rings (Table 1) are present. Therefore, the total lone pair contributions in the  $A_n$  rings fluctuate more than those of the  $(\text{AH})_n$  molecules. However, they are still diatropic and relatively small.

Like the cycloalkanes,<sup>14</sup> the inorganic cycles studied here show remarkable zigzag NICS behavior with ring size. The total  $\sigma$ -bond ring electron count is decisive: 3MRs and 5MRs rings with  $4n + 2$  electrons have lower or even very negative NICSs, whereas 4MRs and 6MRs rings with  $4n$  electrons have higher or even very positive NICSs. The cyclosilanes and the cyclogermans, where the total SiSi and GeGe  $\sigma$ -bond influence is small compared with the omnipresent diatropic SiH and GeH bond contributions, are exceptions. Otherwise, the  $\sigma$ -aromatic/ $\sigma$ -

antiaromatic pattern of the saturated rings follows that of the archetypal cyclic  $\pi$ -conjugated systems; i.e., they can be  $\sigma$ -aromatic or  $\sigma$ -antiaromatic, depending on the total ring electron count.

Dissected NICS confirms that the contributions of the ring  $\sigma$ -bonds are responsible for the zigzag behavior of the total NICS(0) values. The total ring  $\sigma$ -bond contributions of all the molecules studied here and previously<sup>14</sup> show remarkable alternating behavior with ring size. The  $4n + 2/4n$  electron rule, based on the number of ring bond electrons, is followed. The total ring  $\sigma$ -bond contributions of the 3MRs and 5MRs are negative (sometimes very negative), whereas contributions of the 4MRs and 6MRs are less negative (or even quite positive).

The carbon framework of the basic Hückel aromatic  $(\text{CH})_x$  set also exhibits pronounced alternating  $4n + 2$   $\sigma$ -electron behavior: even though all the  $\sigma$ -CC contributions to NICS(0) are paratropic, their magnitude fluctuates.<sup>17</sup> Thus, the IGLO LMO  $\sigma$ -CC NICS(0) totals are +10.2 (cyclopropenium ion), +36.0 (planar cyclobutadiene dication), +10.7 (cyclopentadienyl anion), +13.8 (benzene), and +12.6 (tropylium cation). As noted earlier, these  $\sigma$ -CC contributions reduce the net total diatropic NICS(0) value of benzene and actually contribute most of the paratropic total NICS(0) to cyclobutadiene.<sup>17</sup>

















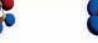





















Some researchers have found that total NICS(0) values of some  $\pi$ -systems do not give the same information as other indices characterizing  $\pi$ -aromaticity/antiaromaticity.<sup>29,30</sup> Instead, the use of NICS(1) or NICS(1)<sub>zz</sub> values greatly improves the agreement between NICS and other aromaticity indices, since the complicating contributions from  $\sigma$ -electrons, although large at the ring center, fall off more rapidly than the contributions of  $\pi$ -electrons.<sup>17</sup> However, for systems where the  $\sigma$ -aromatic/antiaromatic character also is prominent, the inconsistency between NICS indices and other  $\pi$ -electron aromaticity criteria may still exist, especially when the aromaticity/antiaromaticity of the  $\sigma$ - and  $\pi$ -systems are different. NICS indices also include contributions from the paratropic/diatropic  $\sigma$ -ring, while most other indices depend on  $\pi$ -effects and do not respond to  $\sigma$ -aromaticity/antiaromaticity. As we have shown recently, the aromatic 4MR  $\text{C}_4\text{H}_4^{2+}$ , NICS<sub>zz</sub> value is very positive (+35.9) at the ring center (due to the  $\sigma$  effect) and is still +9.4 at 0.5 Å above the ring, while for  $\text{C}_4\text{H}_4^{2-}$  with stronger  $\pi$ -aromaticity, the NICS<sub>zz</sub> value at the ring center is just +8.3 and becomes -11.4 ppm 0.5 Å above the ring.<sup>27</sup>

**Molecular Orbital Analysis.** Examination of the valence MOs of  $\text{S}_n$  rings (Table 1) shows that the  $\sigma$ -type MOs formed primarily by the valence  $\sigma$ -AOs mirror the symmetries of the Hückel orbitals of cyclic  $\pi$ -electron systems (also see ref 31). Hence,  $\sigma$ -aromaticity/ $\sigma$ -antiaromaticity also should follow the  $4n + 2$  and  $4n$  electron rules. The highly symmetrical "radial" Walsh 3MR orbital, formed by p-orbitals pointing inward, is found in all the rings (see Table 1 and ref 31). Cremer proposed in 1988<sup>5b</sup> that this surface-delocalized orbital is largely responsible for the highly  $\sigma$ -aromatic character of cyclopropane. While individual radial orbitals of this type may also be favorable in larger systems, the *total* contributions of all the Walsh-type orbitals in cycloalkanes also show a zigzag trend with increasing ring size.<sup>14</sup> Therefore, the bonding  $\sigma$ -type ring MOs are responsible for the alternating aromatic/antiaromatic behavior of the cyclic saturated molecules. Note that the contributions of the LPs and MH ( $M = \text{Si}, \text{Ge}, \text{N}, \text{P}, \text{As}$ ) bonds always are diatropic.

**Total Strain Energies (TSE).** The strain energies of these saturated cyclic molecules have been studied extensively (see refs 23 and 32 and papers cited). However, many effects



TABLE 1: Valence Molecular Orbitals of the Cyclic  $S_n$  ( $n = 3-6$ ) Molecules<sup>a</sup>

	$D_{3h} S_3$	$D_{2d} S_4$	$C_s S_5$	$D_{3d} S_6$
				
			-0.2356	-0.2570
$\pi$ -type orbitals formed by $p$ -atomic orbitals				
		-0.2247	-0.2605	-0.2764
				
	-0.2441	-0.2740	-0.3048	-0.2953
				
-0.3896	-0.3884	-0.3835	-0.3709	
				
	-0.3776	-0.3645	-0.3676	-0.3534
				
$\sigma$ -type orbitals formed by in-plane $p$ -atomic orbitals			-0.4298	-0.4213
				
	-0.4264	-0.4304	-0.4339	-0.4292
				
		-0.4518	-0.4497	-0.4713
				
			-0.5790	
$\sigma$ -type orbitals formed by $s$ -atomic orbitals				
		-0.5917	-0.6266	-0.6310
				
	-0.6620	-0.7367	-0.8016	-0.7778
				
-0.8922	-0.8831	-0.8865	-0.8810	

<sup>a</sup> The orbital energies are given in hartrees. The MOs are sorted according to their similar features rather than their energies.

contribute to the TSEs, e.g., bond angle deformation, A–H bond strengthening due to rehybridization, 1,3- and torsional interactions, lone pair repulsions, as well as  $\sigma$ -aromaticity and antiaromaticity.<sup>11</sup> As many of these effects should change smoothly with ring size, the zigzag correlations of the total strain energy with ring size can be attributed to the aromatic/antiaromatic contributions.<sup>13</sup>

Note that the cyclic  $(\text{SiH}_2)_n$  and  $(\text{GeH}_2)_n$  behavior is exceptional; their strain energies decrease monotonically with the increase in ring size. The cyclosilane data fit an exponential

decay function (with correlation coefficient 0.993, Figure 5). The very small variations of the  $(\text{SiH}_2)_n$  and  $(\text{GeH}_2)_n$  NICS(1) values in Figure 1 also are exceptional. Silicon and germanium do not rehybridize appreciably<sup>11d</sup> and only exhibit highly attenuated  $\sigma$ -aromaticity/antiaromaticity effects.

This is demonstrated dramatically by comparing the magnitude of the NICS(0) values at the centers of the  $\sigma$ -aromatic cages (Figure 6): compare tetrahedrane ( $-48.3$ ),<sup>14</sup>  $T_d$   $\text{P}_4$  ( $-59.7$ ),<sup>14</sup> and  $T_d$   $\text{As}_4$  ( $-56.0$ )<sup>33</sup> with  $T_d$   $(\text{SiH})_4$  ( $-3.2$ ) and  $(\text{GeH})_4$  ( $+14.8$ ; note the change in sign). The  $\sigma$ -antiaromatic cubane-type cages

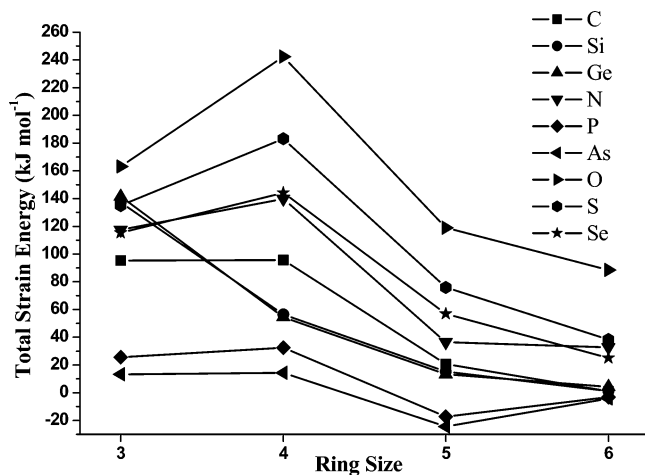


Figure 5. Correlation plot between TSE and ring size.

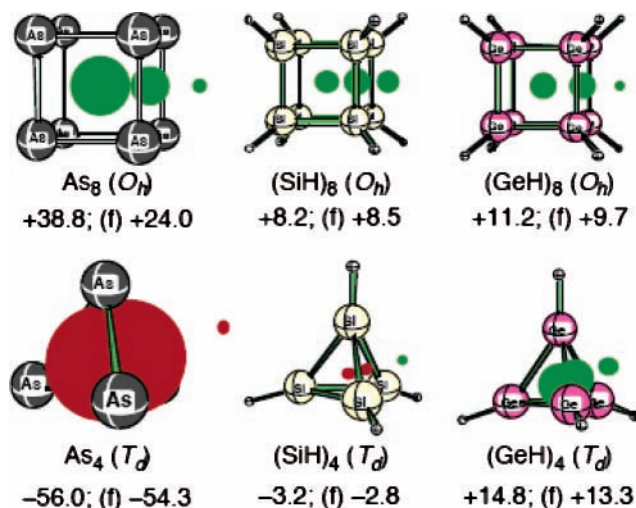


Figure 6.  $\sigma$ -Antiaromatic ( $O_h$ ) and  $\sigma$ -aromatic ( $T_d$ ) saturated inorganic cage IGLO-NICS, including the NICS values at cage centers and at cage faces (f).

behave in the same manner, except that NICS(0) has the opposite sign (Figure 6): cubane (+23.1),<sup>14</sup> cubic  $P_8$  (+43.4),<sup>14</sup> and cubic  $As_8$  (+37.8)<sup>34</sup> may be compared with octasilicubane,  $O_h$   $(SiH)_8$  (+8.2) and  $(GeH)_8$  (+11.2).

Remarkably, the TSEs of the  $\sigma$ -antiaromatic four-membered groups 15 and 16 rings always are *higher* than those of the  $\sigma$ -aromatic three-membered rings, despite the greater angle strain of the latter.  $\sigma$ -Aromatic stabilization seems to be a major contributor to  $(PH)_5$  and  $(AsH)_5$  as well, since their TSEs are *smaller* than those of the corresponding six-membered rings. For  $(CH_2)_5$ ,  $(SiH_2)_5$ ,  $(GeH_2)_5$ ,  $O_5$ ,  $S_5$ , and  $Se_5$  molecules, aromatic stabilization does not dominate the TSE. The TSEs of cyclic  $(GeH_2)_5$  and  $(NH)_5$  are comparable to those of the  $(GeH_2)_6$  and  $(NH)_6$  rings, respectively.

Gimarc et al. have studied the strain energies of main-group homoatomic rings  $[(CH_2)_n, (SiH_2)_n, (NH)_n, (PH)_n, O_n$  and  $S_n$ , with  $n = 3-8$ ] in detail using MP2/6-31G(d) data.<sup>32</sup> They attributed the strain energy maxima found for  $(NH)_4$  and  $(PH)_4$  to lone pair-lone pair repulsions. However, these repulsions are present in all such rings to varying extents. Our examination of the rotational barriers of acyclic models indicates that lone pair repulsions are small. Most recently, Ma et al. explained the unusual stability of  $(PH)_5$ -type rings to the cyclic delocalization of lone pairs through hyperconjugation with the ring PP bonds.<sup>35</sup> As such interactions only are possible in puckered structures, the very large strain energy of  $I_h P_{20}$ , in which all

the five-membered rings are planar, was cited as evidence. However, the strain energies of  $C_{20}H_{20}$ ,  $Si_{20}H_{20}$ ,  $Ge_{20}H_{20}$ , and  $Sn_{20}H_{20}$  are much lower because of the tetrahedral substitution of all the heavy atoms. A recent investigation shows that the high degree of angle strain is a more probable cause of the unusually high strain energy of  $P_{20}$ , where all the PPP angles, constrained to  $108^\circ$ , are widened<sup>36</sup> considerably from the ideal ca.  $90^\circ$  value. Our model computations indicate that this constraint alone would increase the strain energy by over 80 kcal mol<sup>-1</sup>! While  $C_{5v}$   $(PH)_5$ , whose structure resembles that of a  $P_5$  face of  $I_h P_{20}$ , has a  $-8.2$  IGLO-NICS(1) value, the  $P_{20}$  NICS is  $+0.6$  at the cage center and only  $-1.7$  in the center of an angle-deformed  $P_5$  face (GIAO). Hence,  $P_{20}$  lacks aromatic (or antiaromatic) character.

Six-membered rings often are used as "strainless" reference structures for TSE evaluations, but this is not appropriate here. Most of the TSEs for the six-membered rings calculated using homodesmotic reactions 1-3 are *positive*.<sup>23b,32</sup> Our NICS analysis shows that such positive TSEs can be attributed at least in part to  $\sigma$ -antiaromatic destabilization of the 6MRs.

## Conclusions

The zigzag behavior of NICS values and other properties of saturated main group element rings as they increase in size are manifestations of alternating  $\sigma$ -aromaticity and  $\sigma$ -antiaromaticity. This behavior has been demonstrated by dissected NICS analysis of  $A_n$  main group element rings to be due primarily to the interactions of the electrons comprising the ring AA bonds, rather than the AH bonds or the lone pairs. Simple counting of ring  $\sigma$ -bond electrons fits well with the Hückel  $4n + 2/4n$  rule for planar  $\pi$ -systems: three- and five-membered saturated rings are aromatic while four- and six-membered rings are antiaromatic. The symmetries of the  $\sigma$ -ring MOs formed primarily by  $\sigma$ -type atomic orbitals are similar to those of the delocalized  $\pi$ -MOs in planar conjugated rings. Computed strain energies and proton chemical shifts substantiate the existence of  $\sigma$ -aromaticity and  $\sigma$ -antiaromaticity in saturated ring systems.

The accumulating evidence indicates that  $\sigma$ -aromaticity and  $\sigma$ -antiaromaticity extends to cage systems and may be as general as  $\pi$ -aromaticity and  $\pi$ -antiaromaticity of rings. According to the total NICS(0) values in the cage centers, main group tetrahedral molecules, like  $P_4$  and  $As_4$ , are highly aromatic,<sup>14</sup> whereas their cubic  $P_8$ <sup>33</sup> and  $As_8$ <sup>34</sup> counterparts are highly antiaromatic. This conclusion, which supports and extends earlier observations, has significant implications for main group inorganic as well as organic and structural chemistry.

**Acknowledgment.** This work was supported in China by the National Natural Science Foundation (NO. 29892167), Science & Technology Committee of Shanghai Municipal (02DJ14023) as well as the State Key Basic Research Development Program (G2000048009) and in the USA by National Science Foundation Grant CHEM-0209857 as well as the University of Georgia.

**Supporting Information Available:** Energies of species, calculated total strain energies, and NICS values. This material is available free of charge via the Internet at <http://pubs.acs.org>.

## References and Notes

- Minkin, V. I.; Glukhovtsev, M. N.; Smikin, B. Y. *Aromaticity and Antiaromaticity. Electronic and Structural Aspects*; Wiley: New York, 1994.
- Krygowski, T. M.; Cyrański, M. K.; Häeflinger, G.; Katritzky, A. R. *Tetrahedron* **2000**, *56*, 1783-1796.

- (3) (a) Li, X.; Kuznetsov, A. E.; Zhang, H. F.; Boldyrev, A. I.; Wang, L. *S. Science* **2001**, *291*, 859. (b) Kuznetsov, A. E.; Birch, K. A.; Boldyrev, A. I.; Li, X.; Zhai, A. I.; Wang, L. *S. Science* **2003**, *300*, 622.
- (4) (a) Fowler, P. W.; Havenith, R. W. A.; Steiner, E. *Chem. Phys. Lett.* **2001**, *342*, 85. (b) Fowler, P. W.; Havenith, R. W. A.; Steiner, E. *Chem. Phys. Lett.* **2002**, *359*, 530. (c) Juselius, J.; Straka, M.; Sundholm, D. *J. Phys. Chem. A* **2001**, *105*, 9939. (d) Zhan, C. G.; Zheng, F.; Dixon, D. A. *J. Am. Chem. Soc.* **2002**, *124*, 14795. (e) Havenith, R. W. A.; Fowler, P. W.; Steiner, E.; Shetty, S.; Kanhere, D.; Pal, S. *Phys. Chem. Chem. Phys.* **2004**, *6*, 285.
- (5) For example, see: (a) The entire May issue of *Chem. Rev.* **2001**, *105*; Schleyer, P. v. R., special editor. (b) Cremer, D. *Tetrahedron* **1988**, *44*, 7427–7454.
- (6) Chen, Z.; Corminboeuf, C.; Heine, T.; Bohmann, J.; Schleyer, P. v. R. *J. Am. Chem. Soc.* **2003**, *125*, 13930.
- (7) Schleyer, P. v. R.; Maerker, C.; Dransfeld, A.; Jiao, H.; Hommes, N. J. R. v. E. *J. Am. Chem. Soc.* **1996**, *118*, 6317–6318.
- (8) Schleyer, P. v. R.; Jiao, H.; Hommes, N. J. R. v. E.; Malkin, V. G.; Malkina, O. L. *J. Am. Chem. Soc.* **1997**, *119*, 12669–12670.
- (9) (a) Steiner, E.; Fowler, P. W. *J. Phys. Chem. A* **2001**, *105*, 9553. (b) Steiner, E.; Fowler, P. W.; Jenneskens, L. W.; Acocella, A. *Chem. Commun.* **2001**, 659. (c) Steiner, E.; Fowler, P. W.; Jenneskens, L. W.; Havenith, R. W. A. *Eur. J. Org. Chem.* **2002**, *1*, 163. (d) Proft, F. D.; Fowler, P. W.; Havenith, R. W. A.; Schleyer, P. v. R.; Lier, G. V.; Geerlings, P. *Chem. Eur. J.* **2004**, *10*, 940.
- (10) (a) Wannere, C. S.; Schleyer, P. v. R. *Org. Lett.* **2003**, *5*, 865–868. (b) Wannere, C. S.; Moran, D.; Allinger, N. L.; Hess, B. A., Jr.; Schaad, L. J.; Schleyer, P. v. R. *Org. Lett.* **2003**, *5*, 2983–2986.
- (11) (a) Dewar, W. J. S. *J. Am. Chem. Soc.* **1984**, *106*, 669–682. (b) Cremer, D.; Gauss, J. *J. Am. Chem. Soc.* **1986**, *108*, 7467–7477. (c) Wiberg, K. B. *Angew. Chem., Int. Ed. Engl.* **1986**, *25*, 312–322. (d) Exner, K.; Schleyer, P. v. R. *J. Phys. Chem. A* **2001**, *105*, 3407–3416.
- (12) Grev, G. S.; Schaefer, H. F., III. *J. Am. Chem. Soc.* **1987**, *109*, 6569–6577.
- (13) (a) Jiao, H. J.; Schleyer, P. v. R.; Glukhovtsev, M. N. *J. Phys. Chem.* **1996**, *100*, 12299–12304. (b) Jursic, B. S. *Int. J. Quantum Chem.* **1998**, *69*, 679–687. (c) Jursic, B. S. *Int. J. Quantum Chem.* **1999**, *73*, 451–458.
- (14) Moran, D.; Manoharan, M.; Heine, T.; Schleyer, P. v. R. *Org. Lett.* **2003**, *5*, 23–26.
- (15) Jackman, L. M.; Sternhell, S. *Application of Nuclear Magnetic Resonance Spectroscopy in Organic Chemistry*, 2nd ed.; Pergamon: Braunschweig, 1969.
- (16) Havenith, R. W. A.; Fowler, P. W.; Steiner, E. *Chem. Phys. Lett.* **2003**, *371*, 276–283.
- (17) Schleyer, P. v. R.; Manoharan, M.; Wang, Z. X.; Kiran, R.; Jiao, H.; Puchta, R.; Hommes, N. J. R. v. E. *Org. Lett.* **2001**, *3*, 2465–2468.
- (18) With the exception of  $(\text{SiH}_2)_n$  and  $(\text{GeH}_2)_n$ , lone pairs, which might combine to form cyclic  $\pi$ -orbitals, also are present. In particular, the chalogen rings, when planar, have two sets of lone pairs, perpendicular to the ring and in the ring plane. The dissected NICS analysis based on localized orbitals (LMO) assigns these lone pairs, as well as contributions from the ring bonds. The silicon and germanium rings offer a more straightforward LMO NICS analysis, only involving the bonds in the ring and to the hydrogens. The NICS localization of the pycnogen rings involves these bonds and the lone pairs as well. As the most stable conformations of the pycnogen rings have out-of-plane hydrogens, the lone pairs have sp-hybrid character.
- (19) (a) Becke, A. D. *J. Chem. Phys.* **1993**, *98*, 5648–5652. (b) Lee, C.; Yang, W.; Parr, R. G. *Phys. Rev. B* **1988**, *37*, 785–789. (c) Vosko, S. H.; Wilk, L.; Nusair, M. *Can. J. Phys.* **1980**, *58*, 1200–1211. (d) Stephens, P. J.; Devlin, F. J.; Chabalowski, C. F.; Frisch, M. J. *J. Phys. Chem.* **1994**, *98*, 11623–11627.
- (20) Frisch, M. J.; Trucks, G. W.; Schlegel, H. B.; Scuseria, G. E.; Robb, M. A.; Cheeseman, J. R.; Zakrzewski, V. G.; Montgomery, J. A., Jr.; Stratmann, R. E.; Burant, J. C.; Dapprich, S.; Millam, J. M.; Daniels, A. D.; Kudin, K. N.; Strain, M. C.; Farkas, O.; Tomasi, J.; Barone, V.; Cossi, M.; Cammi, R.; Mennucci, B.; Pomelli, C.; Adamo, C.; Clifford, S.; Ochterski, J.; Petersson, G. A.; Ayala, P. Y.; Cui, Q.; Morokuma, K.; Malick, D. K.; Rabuck, A. D.; Raghavachari, K.; Foresman, J. B.; Cioslowski, J.; Ortiz, J. V.; Stefanov, B. B.; Liu, G.; Liashenko, A.; Piskorz, P.; Komaromi, I.; Gomperts, R.; Martin, R. L.; Fox, D. J.; Keith, T.; Al-Laham, M. A.; Peng, C. Y.; Nanayakkara, A.; Gonzalez, C.; Challacombe, M.; Gill, P. M. W.; Johnson, B. G.; Chen, W.; Wong, M. W.; Andres, J. L.; Head-Gordon, M.; Replogle, E. S.; Pople, J. A. *Gaussian98*, revision A.7; Gaussian, Inc.: Pittsburgh, PA, 1998.
- (21) Montgomery, J. A., Jr.; Frisch, M. J.; Ochterski, J. W.; Petersson, G. A. *J. Chem. Phys.* **1999**, *110*, 2822–2827.
- (22) Pople, J. A.; Head-Gordon, M.; Raghavachari, K. *J. Chem. Phys.* **1987**, *87*, 5968–5975.
- (23) (a) George, P.; Trachtman, M.; Bock, C. W.; Brett, A. M. *Tetrahedron* **1976**, *32*, 317. (b) Dudev, T.; Lim, C. *J. Am. Chem. Soc.* **1998**, *120*, 4450–4458.
- (24) Ditchfield, R. *Mol. Phys.* **1974**, *27*, 789–807.
- (25) Kutzelnigg, W.; Fleischer, U.; Schindler, M. In *NMR: Basic Principles and Progress*; Springer: Berlin, 1990; Vol. 23, p 165.
- (26) Malkin, V. G.; Malkina, O. L.; Eriksson, L. A.; Salahub, D. R. *J. Am. Chem. Soc.* **1994**, *116*, 5898–5908.
- (27) Corminboeuf, C.; Heine, T.; Seifert, G.; Schleyer, P. v. R.; Weber, J. *Phys. Chem. Chem. Phys.* **2004**, *6*, 273–276.
- (28) (a) Lazzaretti, P. *Phys. Chem. Chem. Phys.* **2004**, *6*, 217–223. (b) Steiner, E.; Fowler, P. W.; Jenneskens, L. W. *Angew. Chem., Int. Ed.* **2001**, *40*, 362–366.
- (29) (a) Aihara, J. *Chem. Phys. Lett.* **2002**, *365*, 34–39. (b) Aihara, J.; Oe, S. *B. Chem. Soc. Jpn.* **2003**, *76*, 1363–1364. (c) Aihara, J. *B. Chem. Soc. Jpn.* **2004**, *77*, 101–102.
- (30) Poater, J.; García-Cruz, I.; Illas, F.; Solà, M. *Phys. Chem. Chem. Phys.* **2004**, *6*, 314–318.
- (31) Heine, T.; Schleyer, P. v. R.; Corminboeuf, C.; Seifer, G.; Reviakine, R.; Weber, J. *J. Phys. Chem. A* **2003**, *107*, 6470–6475.
- (32) Gimarc, B. M.; Zhao, M. *Coord. Chem. Rev.* **1997**, *158*, 385–412 and references therein.
- (33) Hirsch, A.; Chen, Z.; Jiao, H. *Angew. Chem., Int. Ed.* **2001**, *40*, 2834–38.
- (34) King, R. B.; Schleyer, P. v. R. In *Molecular Clusters of Main Group Elements*; Driess, M., Noeth, H., Eds.; Wiley-VCH: Weinheim, 2004.
- (35) Ma, J.; Hozaki, A.; Inagaki, S. *Inorg. Chem.* **2002**, *41*, 1876–1882.
- (36) Alder, R. W.; Harvey, J. N.; Schleyer, P. v. R.; Moran, D. *Org. Lett.* **2001**, *3*, 3233–3236.